Deriving photospheric parameters and elemental abundances for a sample of stars showing the FIP effect

B. Seli[1,2], L. Kriskovics[1] and K. Vida[1]

[1] *Konkoly Observatory, Research Centre for Astronomy and Earth Sciences, Hungarian Academy of Sciences, 1121 Budapest, Konkoly Thege Miklós út 15-17, Hungary*

[2] *Eötvös University, Department of Astronomy, 1518 Budapest, Pf. 32, Hungary*

Abstract. One puzzling question in solar physics is the difference between elemental abundances in the photosphere and the corona. Elements with low first ionization potential (FIP) can be overabundant in the corona compared to the photosphere under certain circumstances. The same phenomenon has been observed on a handful of stars, while a few of them show the inverse effect. But not all the stars in the original sample had precise photospheric abundances derived from optical spectra, so for some the solar values were adopted. In this work we make homogeneous abundance measurements from optical spectroscopy.

We collected spectra of 16 stars showing the FIP effect with the 1-m RCC telescope of Konkoly Observatory, with resolution of $\lambda/\Delta\lambda \sim 21\,000$. We determine the fundamental astrophysical parameters ($T_{\rm eff}$, $\log g$, $[M/H]$, $\xi_{\rm mic}$, $v\sin i$) and individual elemental abundances with the SME spectral synthesis code using MARCS2012 model atmosphere and spectral line parameters from the Vienna Atomic Line Database (VALD).

Key words: Stars: abundances – Stars: atmospheres – Stars: fundamental parameters – Techniques: spectroscopic

1. Introduction

When working on X-ray spectra, solar physicists found a discrepancy between the abundances of several elements compared to the known photospheric values. In the solar corona, elements with low first ionization potential (FIP) are enhanced by approximately a factor of 4 (Laming, 2015, and references therein). This phenomenon – the FIP effect – was later observed on a handful of stars. The magnitude of the effect shows a spectral type dependence, for stars cooler than K5 the inverse FIP effect was observed, where the low FIP elements are depleted in the corona.

However, for some of these stars the photospheric composition is unknown or the available data were collected from several different sources. Substituting

Table 1. The observed sample. Mean S/N was calculated with the DER_SNR algorithm (Stoehr et al., 2008).

star	number of spectra	S/N	star	number of spectra	S/N
EK Dra	17	77	β Com	5	140
EQ Peg A	24	39	ϵ Eri	42	100
EV Lac	23	23	κ Cet	20	113
GJ 338 A	31	69	ξ Boo A	5	124
GJ 338 B	27	66	ξ Boo B	5	58
Sun	3	99	π^1 UMa	6	143
70 Oph A	5	122	π^3 Ori	40	151
70 Oph B	15	80	χ^1 Ori	35	105

the stellar elemental composition with the solar abundance pattern makes it impossible to determine whether the coronal abundances are caused by the FIP effect or if those elements are just over/underabundant in that particular star. In this work we present new fundamental parameters and elemental abundances derived from new homogeneous optical measurements for stars that are known to show the FIP effect.

2. Data

We selected our target stars showing the FIP effect from Table 2 in Laming (2015). We excluded objects that are not visible from Hungary, as well as faint targets (fainter than $V \sim 8^m$) to ensure sufficient S/N. Our final observed sample consists of 16 main-sequence stars with spectral types ranging from F6 to M3. The full list can be seen in Table 1.

Observations were made with the 1-m RCC telescope of Konkoly Observatory, equipped with an echelle spectrograph with $\lambda/\Delta\lambda \sim 21\,000$ mean resolution. The observations were carried out in March, June, August and November 2017. The quality of most spectra is sufficient for spectral synthesis, while for the fainter stars we have to combine spectra collected on the same night to ensure a high enough S/N.

Data reduction was carried out with the standard IRAF tasks. A ThAr spectral lamp was used for wavelength calibration. 28 echelle orders were extracted from each image uniformly, but we restrict our analysis to the 5000–7000 Å wavelength range, because below 5000 Å the S/N gradually decreases while the region after 7000 Å is dominated by telluric absorption lines.

3. Spectral synthesis

We used the Spectroscopy Made Easy (SME) code (Valenti & Piskunov, 1996) with MARCS2012 model atmosphere to calculate the necessary parameters from the continuum normalized spectra. We downloaded spectral line data from the Vienna Atomic Line Database (VALD; Piskunov et al., 1995) using the "extract stellar" option.

Before fitting the individual elemental abundances, the fundamental parameters of the stars are needed. These are effective temperature ($T_{\rm eff}$), surface gravity ($\log g$), metallicity ([M/H]), microturbulence ($\xi_{\rm mic}$) and projected rotational velocity ($v \sin i$). Another necessary parameter is macroturbulent velocity ($\xi_{\rm mac}$), but since it is hard to disentangle the contribution of $\xi_{\rm mac}$ from the other line broadening effects, we chose to apply the following empirical relation from Valenti & Fischer (2005) rather than fitting $\xi_{\rm mac}$:

$$\xi_{\rm mac} = 3.5 + (T_{\rm eff} - 5777)/650 \qquad (1)$$

The following initial parameters were used: $\log g = 4.5$ dex (since all stars in the sample are dwarfs), $[M/H] = 0$ dex, $\xi_{\rm mic} = 1\,{\rm km\,s^{-1}}$, $v \sin i = 20\,{\rm km\,s^{-1}}$ and $T_{\rm eff}$ inferred from spectral type. In general, no reasonable fit can be achieved if we iterate all parameters at once, so we fit them in the following order: first $\xi_{\rm mic}$ and $v \sin i$ simultaneously, then $T_{\rm eff}$, then $[M/H]$ and $\xi_{\rm mic}$. After this step we fit $\log g$ with a line list containing only the Na D and Mg b lines, since their strong line wings are more sensitive to gravity. Then we proceed by downloading a new line list from VALD with the parameters derived so far. With this we fit $T_{\rm eff}$ once again, then $[M/H]$. The results can be seen in Table 2, and Figure 1 shows an example of the observed and synthetic spectrum of π^3 Ori.

After these steps we fit the individual elemental abundances (along with $[M/H]$), namely C, Na, Mg, Al, Si, S, Ca, Ti, Mn, Fe, Ni and Ba. Some interesting elements whose coronal abundance can be derived from X-ray spectra have no transitions in the observed wavelength range, so their abundances cannot be determined. The result can be seen in Figure 2 for 8 stars from the sample. While most elements show no deviation from the solar scale, there is a clear Ba enhancement for all these stars. According to D'Orazi et al. (2009) young stars tend to have higher Ba abundance, based on empirical results. All stars appearing in Figure 2 are younger than the Sun with the oldest one being β Com with age of ~ 2.5 Gyr, which explains the observed overabundance. To check if any of these 8 stars could be Ba dwarfs we fit other s-process elements, although with larger uncertainties. It turns out that the abundances of La and Ce are high, while the Y and Zr content is approximately solar, which disproves the idea. Al abundances also seem to be higher than solar, but since there are only a few and relatively weak Al lines to fit, it is likely not a real physical effect.
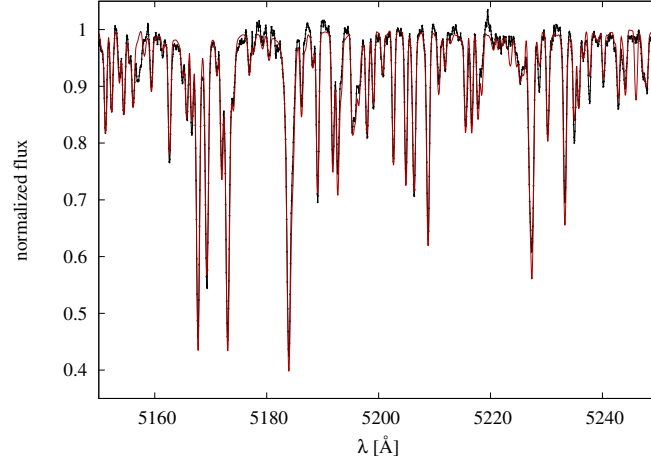
Figure 1. Observed (black) and synthetic (red) spectrum of π^3 Ori near the Mg triplet.

3.1. Error estimation

SME is robust enough to give almost identical results for all spectra collected from the same star on the same night. This means that the standard deviations calculated from multiple observations are small (e.g. 5 K in T_{eff}) and can only be used for consistency check. So the uncertainties of the derived parameters have to be obtained by different means, for example by seeing how much each parameter can be altered before it affects the determination of the other parameters during the fit. The expected average uncertainties are 50 K in T_{eff}, 0.1 dex in $\log g$, 0.1 dex in $[M/H]$, 0.3 km s^{-1} in ξ_{mic} and 3 km s^{-1} in $v \sin i$.

After comparing our results with available literature data, it seems that our $\log g$ values are usually lower by $\sim$0.1 dex. However that should have little effect on the derived abundances. Running the abundance fitting procedure with 0.2 dex difference in $\log g$ modifies the final abundances by $\sim$0.08 dex. 200 K change in T_{eff} results in $\sim$0.07 dex difference, while 0.6 km s^{-1} change in ξ_{mic} gives $\sim$0.05 dex.

4. Conclusion

It appears that a metre-class telescope equipped with a mid-high resolution spectrograph is enough to determine elemental abundances for bright enough stars with the spectral synthesis method. We have collected spectra of 16 stars that show the FIP effect, and carried out the abundance analysis for 8 of them. The remaining stars are the fainter ones with noisier spectra, so for them the
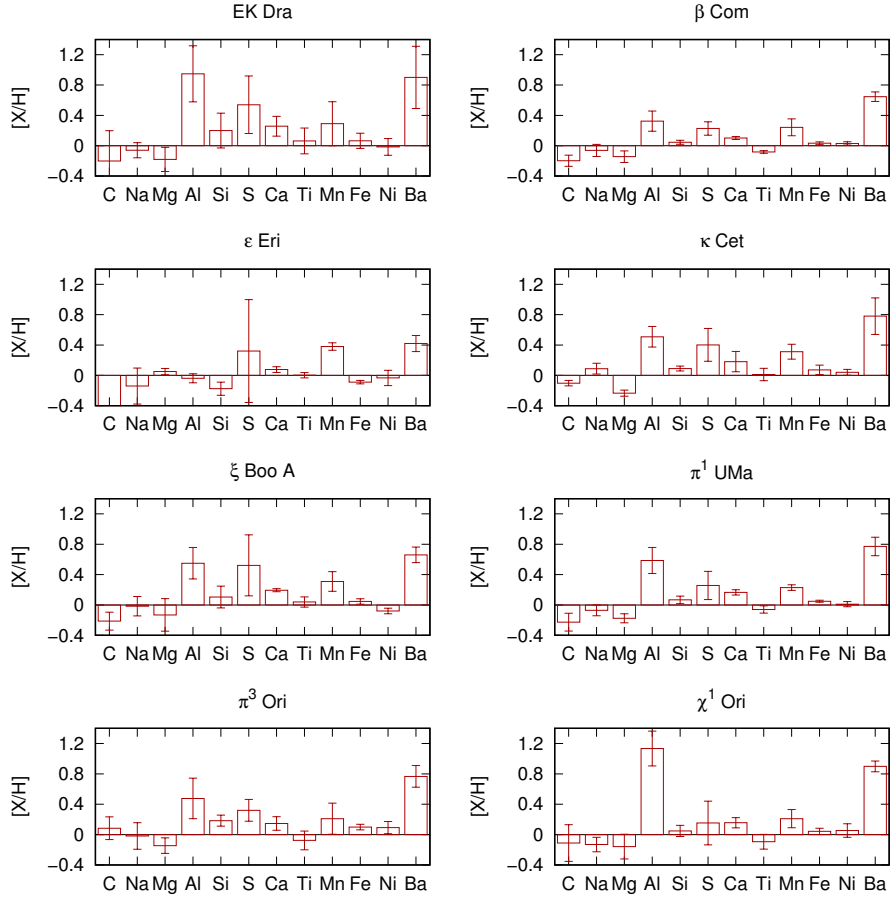
Figure 2. Elemental abundances relative to the solar values (derived in this work). Error bars shown are multiplied by 10 for illustration purposes.

spectral synthesis will be more challenging. In the future we also plan to gather the available X-ray abundances to recalculate the FIP bias for these stars.

Table 2. Fundamental parameters derived from the spectra.

star	T_{eff} [K]	$\log g$ [dex]	$[M/H]$ [dex]	ξ_{mic} [km s^{-1}]	$v \sin i$ [km s^{-1}]
EK Dra	5780	4.46	-0.06	1.32	21.2
β Com	5980	4.37	-0.09	0.92	13.3
ϵ Eri	5150	4.32	-0.07	0.91	12.8
κ Cet	5780	4.39	-0.01	0.83	12.5
ξ Boo A	5670	4.56	-0.16	1.32	14.1
π^1 UMa	5880	4.39	-0.18	0.98	16.9
π^3 Ori	6320	4.37	-0.12	1.06	20.0
χ^1 Ori	5940	4.44	-0.10	0.54	17.2

References

D'Orazi, V., Magrini, L., Randich, S., et al., Enhanced Production of Barium in Low-Mass Stars: Evidence from Open Clusters. 2009, *Astrophys. J.*, **693**, L31, DOI: 10.1088/0004-637X/693/1/L31

Laming, J. M., The FIP and Inverse FIP Effects in Solar and Stellar Coronae. 2015, *Living Reviews in Solar Physics*, **12**, 2, DOI: 10.1007/lrsp-2015-2

Piskunov, N. E., Kupka, F., Ryabchikova, T. A., Weiss, W. W., & Jeffery, C. S., VALD: The Vienna Atomic Line Data Base. 1995, *Astron. Astrophys., Suppl.*, **112**, 525

Stoehr, F., White, R., Smith, M., et al., DER_SNR: A Simple & General Spectroscopic Signal-to-Noise Measurement Algorithm. 2008, in Astronomical Society of the Pacific Conference Series, Vol. **394**, *Astronomical Data Analysis Software and Systems XVII*, ed. R. W. Argyle, P. S. Bunclark, & J. R. Lewis, 505

Valenti, J. A. & Fischer, D. A., Spectroscopic Properties of Cool Stars (SPOCS). I. 1040 F, G, and K Dwarfs from Keck, Lick, and AAT Planet Search Programs. 2005, *Astrophys. J., Suppl.*, **159**, 141, DOI: 10.1086/430500

Valenti, J. A. & Piskunov, N., Spectroscopy made easy: A new tool for fitting observations with synthetic spectra. 1996, *Astronomy and Astrophysics Supplement Series*, **118**, 595